# Characterization and luminescence properties of $Sr_2Si_5N_8:Eu^{2+}$ phosphor for white light-emitting-diode illumination

Xianqing Piao, Takashi Horikawa, Hiromasa Hanzawa, and Ken-ichi Machida[a)]
*Center for Advanced Science and Innovation, Osaka University, 2-1 Yamadaoka, Suita, Osaka 565-0871, Japan*

(Received 8 November 2005; accepted 6 March 2006; published online 18 April 2006)

$Eu^{2+}$-doped ternary nitride phosphor, $Sr_2Si_5N_8:Eu^{2+}$, was prepared by the carbothermal reduction and nitridation method. The Rietveld refinement analysis showed that the single phase products were obtained. Two main absorption bands were observed on the diffuse reflection spectra peaking at about 330 and 420 nm, so that the resultant phosphor can be effectively excited by InGaN light-emitting diodes. The emission peak position of $(Sr_{1-x}Eu_x)_2Si_5N_8:Eu^{2+}$ series varied from 618 to 690 nm with increasing $Eu^{2+}$ ion concentration. The redshift behavior of the emission band was discussed on the basis of the configuration coordination model. © *2006 American Institute of Physics*. [DOI: 10.1063/1.2196064]

InGaN-based white light-emitting diodes (LEDs) have drawn much attention due to their valuable applications, such as backlighting source for liquid crystal displays and power saving illumination supply units for the substitute for incandescent lamps.[1] The $Y_3Al_5O_{12}:Ce^{3+}$ material has already been used as the yellow phosphor for the white LED because the luminescence efficacy (25 lm/W at a forward bias of 20 mA) and the color rendering index ($R_a \sim 85$) are enough for the general illumination. However, without containing any red light component, the "white" output light cannot realize the desirable color balance for a true color rendition. Consequently, the low $R_a$ value in the low color-temperature area has limited the possible applications of white LED, such as uses in the medical and architectural lighting fields. There are alternative ways to generate warm white lights: one is to combine an UV chip with red, green, and blue (RGB) phosphors[2] and another one is to compensate the red deficiency of yttrium aluminum garnet (YAG):$Ce^{3+}$-based LED with a separate red light.[3] Among all candidates for the red phosphors, the tetrahedral $SiN_4$-based nitrides show much promising potential compared with sulfide phosphor owing to their high thermal and chemical stability and excellent photoluminescence properties. In the past several years, however, only a few numbers of nitridosilicates have been synthesized due to the scarcity of appropriate synthesis methods. The reason is ascribed to the inert property of $Si_3N_4$ even at high temperature, as well as the oxygen and moisture sensitivity of alkaline earth metals and nitrides as starting materials. To some extent this obstacle has been overcome by Schnick and co-workers.[4,5] They employed a synthetic approach based on the reaction of various metals with silicon diimide $Si(NH_2)$. Consequently, a series of ternary $M$–Si–N or quaternary $M$–Ln–Si–N nitrides ($M$=alkaline earths, Ln=rare earths) have been successfully prepared. However, this method is not suitable for mass production owing to the limitation of high cost and sensitivity of raw materials.

In the present work, we synthesized a series of $(Sr_{1-x}Eu_x)_2Si_5N_8$ compounds by employing the carbothermal reduction and nitridation (CRN) method, and the resultant powder samples were characterized for the application as a red phosphor for white LEDs. Stoichiometric amounts of $SrCO_3$ (99.99%), $Si_3N_4$ (99.5%), $Eu_2O_3$ (99.99%), and fine graphite powder (99.9%) were mixed thoroughly and pressed into a graphite crucible positioned in a radio frequency (rf) furnace for a two-step heating under $N_2$ gas flow. Firstly, the mixture was heated at 1473 K for 2 h to decompose $SrCO_3$ completely, and then the temperature was increased to 1773 K and maintained for 6 h to form the $(Sr_{1-x}Eu_x)_2Si_5N_8$ phosphors. Under the strong reducing atmosphere, SrO and $Eu_2O_3$ were reduced to corresponding metals, and at the same time, they were completely nitrogenized and then reacted with the silicon nitride. The total reaction was as follows:

$$Eu_2O_3 + SrO + C + N_2 + Si_3N_4 \rightarrow (Sr_{1-x}Eu_x)_2Si_5N_8 + CO\uparrow. \quad (1)$$

The structure was checked by x-ray powder diffraction (RINT2200, Rigaku) with Cu $K\alpha$ radiation. Diffuse reflection spectra were obtained by a $BaSO_4$ powder calibrated UV-visible spectrophotometer (UV-2200, Shimadzu). The photoluminescence spectra were measured using fluorescent spectrophotometers (Hitachi F-4500 at room temperature and Ocean 2000 at liquid He cooling system). The oxygen content was measured by an O/N analyzer (EMGA-550, Horiba).

The obtained $(Sr_{1-x}Eu_x)_2Si_5N_8$ series samples are all indexed by the $Sr_2Si_5N_8$ phase (JCPDS 85-0101). The Rietveld analysis for the sample with a composition of $(Sr_{0.98}Eu_{0.02})_2Si_5N_8$ is carried out by using FULLPROF (Ref. 6) software as shown in Fig. 1. The structure refined to $R_p$=6.26% and $R_{wp}$=9.88% [$Pmn2_1$, $a$=571.57(7) pm, $b$=681.11(7) pm, and $c$=934.99(2) pm] is in good agreement with the previous work.[4] The refinement results show that the occupation of Sr atom (~0.95) is lower than that of the theoretical value (~0.98). It means that some amount of Sr component is evaporated at high temperature. Also, the oxygen content about 2 wt % is detected by an O/N analyzer. Obviously, the charge imbalance caused by $Sr^{2+}$ ion vacancy ($V_{Sr}$) is compensated by introduction of the substitutional oxygen ($O_N$). The oxygen content of phosphor is considerably suppressed to less than 0.5 wt % by adding

[a)]Electronic mail: machida@casi.osaka-u.ac.jp

 

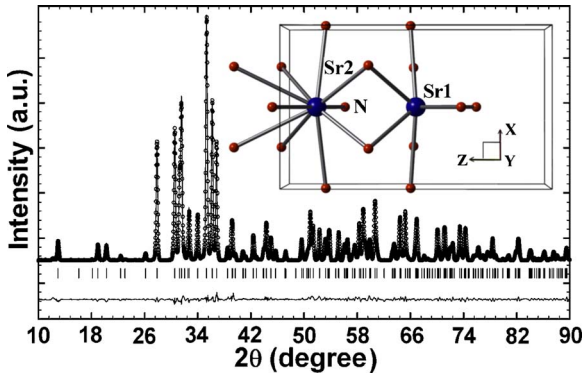


FIG. 1. (Color online) Observed (circle) and calculated (line) XRD patterns as well as the difference (bottom line) between them. Bragg positions are shown as vertical bars. The inset shows the coordination of two $Sr^{2+}$ ion sites along [010].

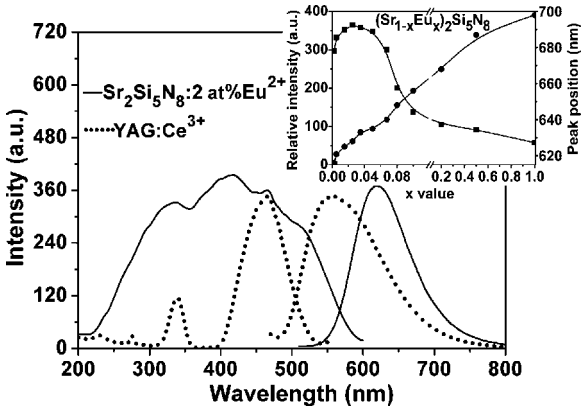


FIG. 3. Typical photoluminescence spectra of $Sr_2Si_5N_8:Eu^{2+}$ (2 at. %) and $YAG:Ce^{3+}$. The inset shows the dependence of emission intensity and peak position of $(Sr_{1-x}Eu_x)_2Si_5N_8$ phosphors on $Eu^{2+}$ concentration.

10% excess of $SrCO_3$. In $Sr_2Si_5N_8$ host, the $Eu^{2+}$ ions take the sites of $Sr^{2+}$ ions which are arranged in the channels formed by $Si_6N_6$ rings along the [100] orientation. As shown in the inset of Fig. 1, two kinds of $Sr^{2+}$ ion sites, Sr1 and Sr2, can be occupied by the $Eu^{2+}$ ions.[4] According to the structure analysis made in this work, they have the coordination numbers of 8 and 10, respectively. The mean distance of Sr1–N [2.865(6)] is smaller than that of Sr2–N [2.928(7)], so that the $Eu^{2+}$ ions substituting the Sr1 site experience stronger crystal field strength which is inversely proportional to $R^5$ ($R$: chemical bond length between a cation with $d$ orbital electrons and the coordinating anion).[7]

Figure 2 shows diffuse reflection spectra of $Sr_2Si_5N_8:Eu^{2+}$ phosphors with different $Eu^{2+}$ ion concentrations. For all samples, two absorption bands peaking at 330 and 420 nm in the UV-visible region are observed, of which the first one is caused by the absorption of host and the second by the absorption $4f^7 \rightarrow 4f^6 5d$ transition of $Eu^{2+}$ ion. With increasing $Eu^{2+}$ ion concentration, the absorption is intensified and the band edge extends to the longer wavelength, which yield the daylight color of samples ranging from orange to dark red.

Typical photoluminescence spectra of the $Sr_2Si_5N_8:Eu^{2+}$ (2 at. %) phosphor, together with that of standard $YAG:Ce^{3+}$ (P46-Y3) as comparison, are shown in Fig. 3. The broad excitation spectrum covers the wavelength range from UV to visible area and consists of two broad bands. The first band peaking at 250–350 nm is ascribed to the transition between the valence and conduction bands of the host. The excitation energy can be transferred nonradiatively from the host to the activator to emit red light. Another band situated in the range of 350–600 nm is responsible for the direct excitation of $Eu^{2+}$ ion ($4f^7 \rightarrow 4f^6 5d$). The emission spectrum at the excitation of 450 nm shows a broadband (FWHM ~ 92 nm) peaking at 620 nm which is assigned to the allowed $4f^6 5d^1 \rightarrow 4f^7$ transition of $Eu^{2+}$ ion. Compared with $MF_2:Eu^{2+}$ and $M_2SiO_4:Eu^{2+}$ ($M$=Sr/Ba), the emission of $Sr_2Si_5N_8:Eu^{2+}$ phosphor occurs at fairly longer wavelength. It can be attributed to the higher electronegativity and nephelauxetic effect of $N^{3-}$ ion, which effectively lower the gravity center of $5d$ orbitals of $Eu^{2+}$ ion.[8] The emission intensity of optimized $Sr_2Si_5N_8:Eu^{2+}$ (2 at. %) phosphor is about 107% of $YAG:Ce^{3+}$ at the same excitation of 450 nm. Dependence of peak position and emission intensity on $Eu^{2+}$ ion concentration is shown in the inset of Fig. 3. With increasing $Eu^{2+}$ ion content, the emission intensity is maximized at the concentration around 2 at. % of $Eu^{2+}$ ion doping and then decreases sharply by doping the higher $Eu^{2+}$ concentration than 6 at. % due to the concentration quenching effect. Also, the emission peak position of $Sr_2Si_5N_8:Eu^{2+}$ redshifts from 618 to 690 nm by increasing $Eu^{2+}$ ion content.

The above luminescence properties, viz., the redshift and the concentration quench of $Sr_2Si_5N_8:Eu^{2+}$ emission, are elucidated according to the schematic configuration coordination model [Fig. 4(a)]. Since $Eu(Sr2)^{2+}$ and $Eu(Sr1)^{2+}$ ions

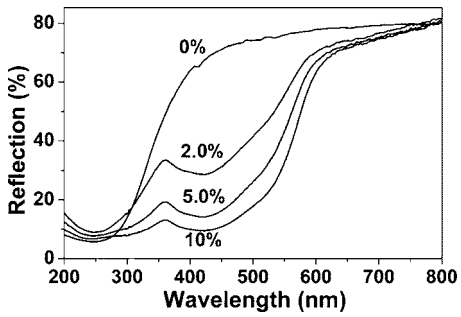


FIG. 2. Diffuse reflection spectra of $(Sr_{1-x}Eu_x)_2Si_5N_8$ phosphors with $x$=0, 0.02, 0.05, and 0.1.

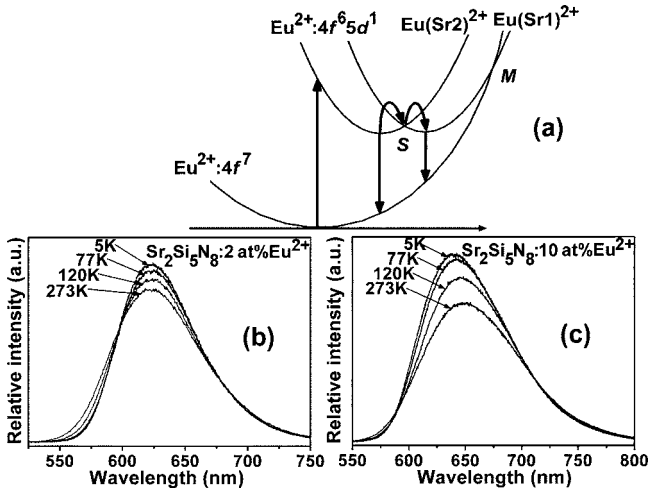


FIG. 4. The configuration coordination model for the $Eu(Sr1)^{2+}$ and $Eu(Sr2)^{2+}$ ions (a) and the temperature dependence of emission bands of $(Sr_{1-x}Eu_x)_2Si_5N_8$ samples with $x$=0.02 (b) and 0.10 (c), respectively.

in $Sr_2Si_5N_8:Eu^{2+}$ phosphor experience different crystal field strengths, the $4f^65d^1$ excited states of them are located at different energy levels and lead to the transition to the ground state with different energy values. The dopant $Eu^{2+}$ ions usually prefer the loose environment of Sr2 site, so that in the low $Eu^{2+}$ ion concentration region the emission peak locates at the higher energy side of the spectrum.[9] In this case, the $Eu(Sr2)^{2+}$ ions serve as the main luminescent center. This is supported by temperature-dependent emission spectra of $Sr_2Si_5N_8:Eu^{2+}$ with the doping concentration of 2 and 10 at. % [Figs. 4(b) and 4(c)]. For the sample of $Sr_2Si_5N_8:Eu^{2+}$ (2 at. %), the emission band peaking at 620 nm has almost no shift when temperature increases from 5 to 273 K, only the emission intensity is decreased by 13.0% of the initial value. However, the emission intensity of $Sr_2Si_5N_8:Eu^{2+}$ (10 at. %) is considerably decreased (by about 25.5%) and the peak position redshifted about 235.8 $cm^{-1}$ at the same temperature range. This means that the interatomic distance between $Eu^{2+}$ ions is shortened by increasing $Eu^{2+}$ ion concentration and then energy transfer occurs much frequently through the multipolar interaction, so that the temperature quenching becomes so significant for the $Sr_2Si_5N_8:Eu^{2+}$ (10 at. %) sample. That is, the electron is easily transferred from the $Eu(Sr2)^{2+}$ ion to $Eu(Sr1)^{2+}$ ion through the intersection of *S* point by overcoming the energy barrier and finally reverts to the ground state to give a longer wavelength emission. The probability of an electron making the transition via point *S* is generally given by[10]

$$\alpha = s \exp\left(\frac{-\Delta E}{kT}\right), \tag{2}$$

where *k* is the Boltzmann constant and *s* is the frequency factor. This transition is strongly dependent on the energy barrier $\Delta E$ and temperature *T*. The probability $\alpha$ generally increases with increasing the measurement temperature. This can be observed from the temperature dependence of emission band for $Sr_2Si_5N_8:Eu^{2+}$ (10 at. %). Additionally, the $4f$ electron in the excited state crosses the intersection point between the $4f^65d$ and $4f^7$ states of $Eu^{2+}$ ion through thermal phonon assisting and returns to the ground state nonradiatively. As the position of intersection point of $Eu(Sr2)^{2+}$ is located at higher energy level than that of $Eu(Sr1)^{2+}$, the more electrons are expected to be transferred from $4f^65d^1$ state of $Eu(Sr1)^{2+}$ to the ground state than that of $Eu(Sr2)^{2+}$ ion. Therefore, with increasing the $Eu^{2+}$ ion concentration, the probability of nonradiative transition is also increased leading to more decrease of emission intensity for $Sr_2Si_5N_8:Eu^{2+}$ (10 at. %) sample.

The Commission Internationale del'Eclairage (CIE) 1931 chromaticity of $(Sr_{1-x}Eu_x)_2Si_5N_8$ phosphors is shown in Fig. 5(a). The chromaticity index $(x,y)$ shifts from (0.621,0.368) to (0.669,0.322) by varying the $Eu^{2+}$ ion content from 2 to 50 at. %, while the chromatic coordinates of

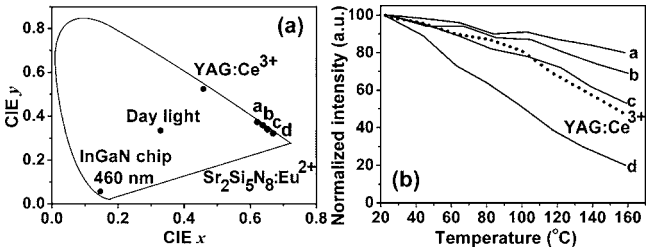


FIG. 5. (a) CIE chromaticity coordinates and (b) temperature quenching of the $(Sr_{1-x}Eu_x)_2Si_5N_8$ samples with $x=0.02$ (a), 0.05 (b), 0.10 (c), and 0.5 (d).

YAG:$Ce^{3+}$ is (0.461, 0.525). The characteristic index shows that these red emission $Sr_2Si_5N_8:Eu^{2+}$ phosphors have high color saturation. In addition, one can see from Fig. 5(b) that the optimized $Sr_2Si_5N_8:Eu^{2+}$ (2 at. %) phosphor has comparatively low temperature quenching effect. With increasing temperature up to 150 °C, the normalized emission intensity of $Sr_2Si_5N_8:Eu^{2+}$ (2 at. %) is decreased to 80% of the initial value, whereas 60% for the YAG:$Ce^{3+}$ (P46-Y3) phosphor. Since the $Sr_2Si_5N_8:Eu^{2+}$ phosphor is efficiently excited at blue lights in the range of 450–470 nm which matches perfectly with the InGaN-LEDs, it can be used to compensate the red color deficiency of YAG:$Ce^{3+}$-based white LEDs or to create white light by combining with a blue chip and another green phosphor.

In conclusion, the excellent red phosphors, $Sr_2Si_5N_8:Eu^{2+}$, of which the oxygen impurity content is effectively lowered below 1.0 wt %, are prepared by the CRN method. The powder samples doped with $Eu^{2+}$ ion at the optimized concentration of 2 at. % (versus $Sr^{2+}$ site) is efficiently excited by the blue light (400–460 nm) of InGaN-based LEDs and the emission intensity is competitive with that of YAG:$Ce^{3+}$ (P46-Y3). In addition, the emission peak position (625 nm) and the chromaticity index of (0.621,0.368) show that this efficient phosphor can be used as a potential candidate for the phosphor-converted white LEDs.

[1] S. Nakamura and G. Fasol, *The Blue Laser Diode* (Springer, Berlin, 1996).
[2] Y. Narukawa, I. Niki, K. Izuno, M. Yamada, Y. Murazaki, and T. Mukai, Jpn. J. Appl. Phys., Part 2 **41**, L371 (2002).
[3] M. Yamada, T. Naitou, K. Izuno, H. Tamaki, Y. Murazaki, M. Kameshima, and T. Mukai, Jpn. J. Appl. Phys., Part 2 **42**, L20 (2003).
[4] T. Schlieper, W. Milius, and W. Schnick, Z. Anorg. Allg. Chem. **621**, 1380 (1995).
[5] W. Schnick, R. Bettenhausen, B. Götze, H. Huppertz, E. Irran, S. Rannabauer, and F. Wester, Z. Anorg. Allg. Chem. **629**, 902 (2003).
[6] T. Roisnel and J. Rodríguez-Carvajal, *Proceedings of the Seventh European Powder Diffraction Conference (EPDIC 7), Barcelona, Spain, 20–23 May 2000*, edited by R. Delhez and E. J. Mittemeijer [Mater. Sci. Forum **378–381**, 118 (2001)].
[7] T. Kanou, *Handbook of Phosphors* (Ohm, Tokyo, 1987).
[8] G. Blasse and B. C. Grabmaier, *Luminescent Materials* (Springer, Berlin, 1994).
[9] H. A. Höppe, H. Lutz, P. Morys, W. Schnick, and A. Seilmeier, J. Phys. Chem. Solids **61**, 2001 (2000).
[10] S. Shionoya and W. M. Yen, *Phosphor Handbook* (CRC, New York, 1999).